CORONAVIRUS

Systemic and mucosal immune profiling in asymptomatic and symptomatic SARS-CoV-2–infected individuals reveal unlinked immune signatures

Supriya Ravichandran†, Gabrielle Grubbs†, Juanjie Tang†, Youri Lee†, Chang Huang, Hana Golding, Surender Khurana*

Mucosal immunity plays a key role in prevention of SARS-CoV-2 virus spread to the lungs. In this study, we evaluated systemic and mucosal immune signatures in asymptomatic SARS-CoV-2–infected versus symptomatic COVID-19 adults compared with RSV-infected adults. Matched serum and nasal wash pairs were subjected to cytokine/chemokine analyses and comprehensive antibody profiling including epitope repertoire analyses, antibody kinetics to SARS-CoV-2 prefusion spike and spike RBD mutants, and neutralization of SARS-CoV-2 variants of concern. The data suggest independent evolution of antibody responses in the mucosal sites as reflected in differential IgM/IgG/IgA epitope repertoire compared with serum. Antibody affinity against SARS-CoV-2 prefusion spike for both serum and nasal washes was significantly higher in asymptomatic adults compared with symptomatic COVID-19 patients. Last, the cytokine/chemokine responses in the nasal washes were more robust than in serum. These data underscore the importance of evaluating mucosal immune responses for better therapeutics and vaccines against SARS-CoV-2.

INTRODUCTION

Mucosal immunity plays an important role in control of respiratory viral infections. In addition to systemic immune responses against the severe acute respiratory syndrome coronavirus 2 (SARS-CoV-2), more emphasis is required to study of mucosal immunity in the nasal cavity, which is the route of virus infection and site of early virus replication. Mucosal antibody response may be important in the fight against infections in the upper respiratory tract, including those by coronaviruses, and could block virus infection of epithelial cells (*1*). Recent publications suggested detection of spike-specific immunoglobulin A (IgA) in saliva and nasal washes of symptomatic coronavirus disease 2019 (COVID-19) patients, but the levels were much lower than in the serum and correlated with viral loads and disease severity (*2*–*4*).

Enzyme linked immunosorbent assay (ELISA) and neutralization tests have primarily been used to characterize antibody responses in human plasma following SARS-CoV-2 infection but provide minimal insight into the diversity and quality of polyclonal antibody responses across the SARS-CoV-2 spike in COVID-19 patients (*5*, *6*). Moreover, there is limited knowledge about the mucosal antibody repertoire of post–SARS-CoV-2 infection, especially in asymptomatic individuals who may be the driver of the ongoing COVID-19 pandemic (*7*). Therefore, in-depth immune profiling of systemic versus mucosal antibody responses in asymptomatic versus symptomatic SARS-CoV-2–infected individuals compared with age-matched respiratory syncytial virus (RSV)–infected adults is important for a better understanding of the host humoral immune response at the site of SARS-CoV-2 exposure and initial viral replication, which could inform risk mitigation strategies and development and evaluation of vaccines and therapeutics against SARS-CoV-2.

Division of Viral Products, Center for Biologics Evaluation and Research (CBER), FDA, Silver Spring, MD 20993, USA.
*Corresponding author. Email: surender.khurana@fda.hhs.gov
†These authors contributed equally to this work.

We used the unbiased, comprehensive approach of Genome Fragment Phage Display Library (GFPDL) technology that was earlier used to elucidate both linear and conformational antibody epitope repertoire following vaccination or infection with viruses including SARS-CoV-2, influenza virus, Zika virus, RSV, and Ebola virus (*8*–*12*). In a recent study of RSV-infected individuals, we observed substantial differences in the specificity of antibodies, antibody isotypes distribution, and antibody affinity between nasal washes and serum antibodies (*13*). Therefore, it is important to compare the immune responses at the mucosal sites with systemic antibody responses to better understand the kinetics, specificity, and antibody affinity following SARS-CoV-2 infection in asymptomatic versus symptomatic COVID-19 adults and to compare them with RSV-infected adults.

In the current study, we performed comprehensive evaluation of SARS-CoV-2 humoral immune response in 15 paired serum/nasal wash samples obtained from SARS-CoV-2 polymerase chain reaction (PCR)–confirmed asymptomatic adults versus time-matched 11 paired serum/nasal wash samples obtained from SARS-CoV-2 PCR-confirmed symptomatic COVID-19 adults (10 days after PCR confirmation) and, as controls, age-matched 15 serum/nasal wash samples from RSV-infected adults. IgM/IgG/IgA antibody epitope repertoires were identified using SARS-CoV-2 spike GFPDL. Surface plasmon resonance (SPR) was used to measure the antibody binding kinetics of paired sera and nasal washes to the stabilized SARS-CoV-2 prefusion spike and spike receptor binding domain (RBD) representing original strain USA-WA1/2020 (WA-1) as well as RBD mutants engineered to express key amino acid mutations from the variants of concern (VOCs).

To probe the innate response to SARS-CoV-2 infection, we measured the cytokine milieu in the serum and nasal washes of these asymptomatic versus symptomatic SARS-CoV-2–infected individuals versus RSV-infected adults. Our findings underscore the importance of evaluating the mucosal immune profile in addition to the systemic immune response following SARS-CoV-2 infection to obtain a better understanding of the respiratory tract immune status, which could inform strategies to control the COVID-19 disease manifestations.

RESULTS

Cytokine and chemokine profiling of serum and nasal washes matched pairs from asymptomatic versus symptomatic SARS-CoV-2– and RSV-infected adults

In the current study, three sets of paired serum and nasal washes were evaluated: 15 asymptomatic SARS-CoV-2–infected males (age ranging from 21 to 55 years) who were diagnosed as SARS-CoV-2 PCR positive on 29 July 2020, samples were collected 10 days later (9 August 2020), all of them were still asymptomatic; 11 symptomatic hospitalized COVID-19 males (age ranging from 26 to 71 years) who were diagnosed as SARS-CoV-2 PCR positive in August to November 2020, and serum/nasal wash paired samples were collected 10 days after the day of PCR confirmation. As controls, we used paired serum/nasal washes from 15 age-matched symptomatic RSV-infected nonhospitalized normal males (age ranging from 21 to 57 years) collected in 2015 (table S1).

Elevated plasma levels of proinflammatory cytokines were reported for symptomatic COVID-19 patients (*14*, *15*). Therefore, to probe the local mucosal and systemic innate immunity, we investigated the levels of cytokines/chemokines in the serum and nasal washes from the asymptomatic and symptomatic SARS-CoV-2–infected individuals in comparison with similar matched sample pairs from RSV-infected adults. Serum samples from symptomatic COVID-19 patients demonstrated higher levels of interleukin-8 (IL-8), eotaxin, fms-related tyrosine kinase 3 (FLT3) ligand, and fractalkine compared with the asymptomatic SARS-CoV-2 serum samples (Fig. 1A, tables S2 and S3, and fig. S1).

The nasal washes in all groups demonstrated overall high levels of cytokines and chemokines (Fig. 1B, tables S2 and S3, and fig. S1). IL-1β and granulocyte colony-stimulating factor (G-CSF) were elevated in the nasal washes of asymptomatic individuals. On the other hand, nasal washes from symptomatic COVID-19 patients contained higher levels of interferon-α (IFN-α), IL-6, IL-8, monocyte chemoattractant protein-1 (MCP-1), macrophage inflammatory protein-3 (MIP-3α), FLT3 ligand, fractalkine, interferon gamma-induced protein 10 (IP-10), platelet-derived growth factor AA (PDGF-AA), and tumor necrosis factor–related apoptosis-inducing ligand (TRAIL) (was also elevated in nasal washes of symptomatic RSV patients) compared with nasal washes from asymptomatic SARS-CoV-2–infected individuals (Fig. 1B, tables S2, and fig. S1). These results suggest a robust local cytokine/chemokine response in the upper respiratory tract of SARS-CoV-2–infected patients, resembling RSV patients that are involved in recruitment of inflammatory cells (neutrophils and macrophages) and promotion of local inflammation and cell apoptosis at the mucosal site of SARS-CoV-2 replication.

IgM, IgG, and IgA antibody epitope repertoires in paired serum and nasal washes from asymptomatic versus symptomatic SARS-CoV-2–infected adults using SARS-CoV-2 spike GFPDL

To elucidate the antibody epitope repertoire in an unbiased manner, the matched serum-nasal wash paired samples were analyzed with a highly diverse SARS-CoV-2 spike GFPDL displaying epitopes of 18– to 500–amino acid residues with $>10^{7.1}$ unique phage clones across the SARS-CoV-2 spike. As part of GFPDL characterization, we mapped the conformation-dependent epitopes of monoclonal antibodies targeting SARS-CoV-2. Previously, we demonstrated that SARS-CoV-2 GFPDL recognizes linear, conformational, and neutralizing epitopes following SARS-CoV-2 infection in humans (*12*, *16*) and postvaccination rabbit sera (*11*). Moreover, in the current study, we subjected pooled sera and pooled nasal washes to adsorption with the SARS-CoV-2 spike GFPDL and demonstrated >95% removal of spike-binding IgM/IgG/IgA antibodies in an ELISA (fig. S2). Therefore, the SARS-CoV-2 spike GFPDL, which expresses both large and short sequences, is capable of presenting epitopes recognized by most of the spike-specific antibodies. However, this SARS-CoV-2 spike GFPDL is not likely to display rare quaternary epitopes formed by cross-protomers on spike trimer or glycosylation-dependent epitopes.

Equal volumes of pooled human serum samples or nasal washes were used for GFPDL panning followed by anti-Ig selection in-solution using anti-IgM, protein A/G (IgG), or anti-IgA specific affinity resins as previously described (*8*–*13*). Two independent panning of pooled sera and nasal washes from symptomatic versus asymptomatic patients were conducted in a blinded fashion. The antibody-bound phages by isotype-specific reagents (IgM, IgG, and IgA) and the individual phages were sequenced and aligned to the SARS-CoV-2 spike to map the global pattern of epitope recognition following SARS-CoV-2 infection (Fig. 2 and figs. S3 and S4 for asymptomatic and symptomatic SARS-CoV-2 cohort, respectively).

In asymptomatic individuals, similar number of phages were bound by serum and nasal wash IgA antibodies (~2×10^4), while the IgM- and IgG-bound phages by the pooled nasal washes (7×10^3 and 1.9×10^3, respectively) were 5- to 100-fold lower compared with serum IgM and IgG antibodies (~2×10^4 and 2×10^5, respectively) (fig. S3A). In the case of asymptomatic nasal washes, IgA bound much higher phages than either IgM or IgG antibodies (fig. S3A).

A similar GFPDL analysis was conducted on the matched pooled sera and nasal washes from symptomatic COVID-19 patients (Fig. 2 and fig. S4). Again, 10-fold more phages were bound by serum IgG (3.5×10^5) compared with IgM and IgA serum antibodies (~2.0×10^4). Unexpectedly, the number of phages bound by IgG in the nasal washes of symptomatic patients was 100-fold higher than IgA-bound clones (2×10^4 versus 2×10^2, respectively) (fig. S4A). In contrast, serum samples from RSV infections bound very few SARS-CoV-2 spike GFPDL phages (fig. S5). The complete mapping of the phage clones bound by IgM, IgG, and IgA in the pooled sera and nasal washes from the asymptomatic versus symptomatic SARS-CoV-2 infections is depicted in Fig. 2 and figs. S3B and S4B, respectively. Mucosal IgA in pooled nasal wash from asymptomatic individuals bound 68-fold higher phage clones than IgA in pooled nasal wash in symptomatic COVID-19 patients (fig. S3A versus fig. S4A), suggesting a robust local IgA response in asymptomatic SARS-CoV-2–infected individuals.

The IgM, IgG, and IgA antibodies in serum and nasal washes of asymptomatic and symptomatic COVID-19 adults (10 days after SARS-CoV-2 confirmation) demonstrated a diverse epitope repertoire spanning the entire spike protein including N-terminal domain (NTD) and RBD in S1 and the fusion peptide (FP), β-rich connector domain, heptad repeat 1 (HR1), and HR2 in S2 (Fig. 2 and figs. S3 and S4). In contrast, the very few phage clones bound by pooled sera from RSV patients (fig. S5) primarily recognized the S1-NTD, C terminus of S1, and N terminus of S2, which may represent antibodies against conserved regions between seasonal coronaviruses and SARS-CoV-2 spike (*17*, *18*).

Most of the antigenic sites identified following SARS-CoV-2 infection (length ranging from 36– to 249–amino acid residues) were recognized by antibodies in both serum and nasal wash. However,

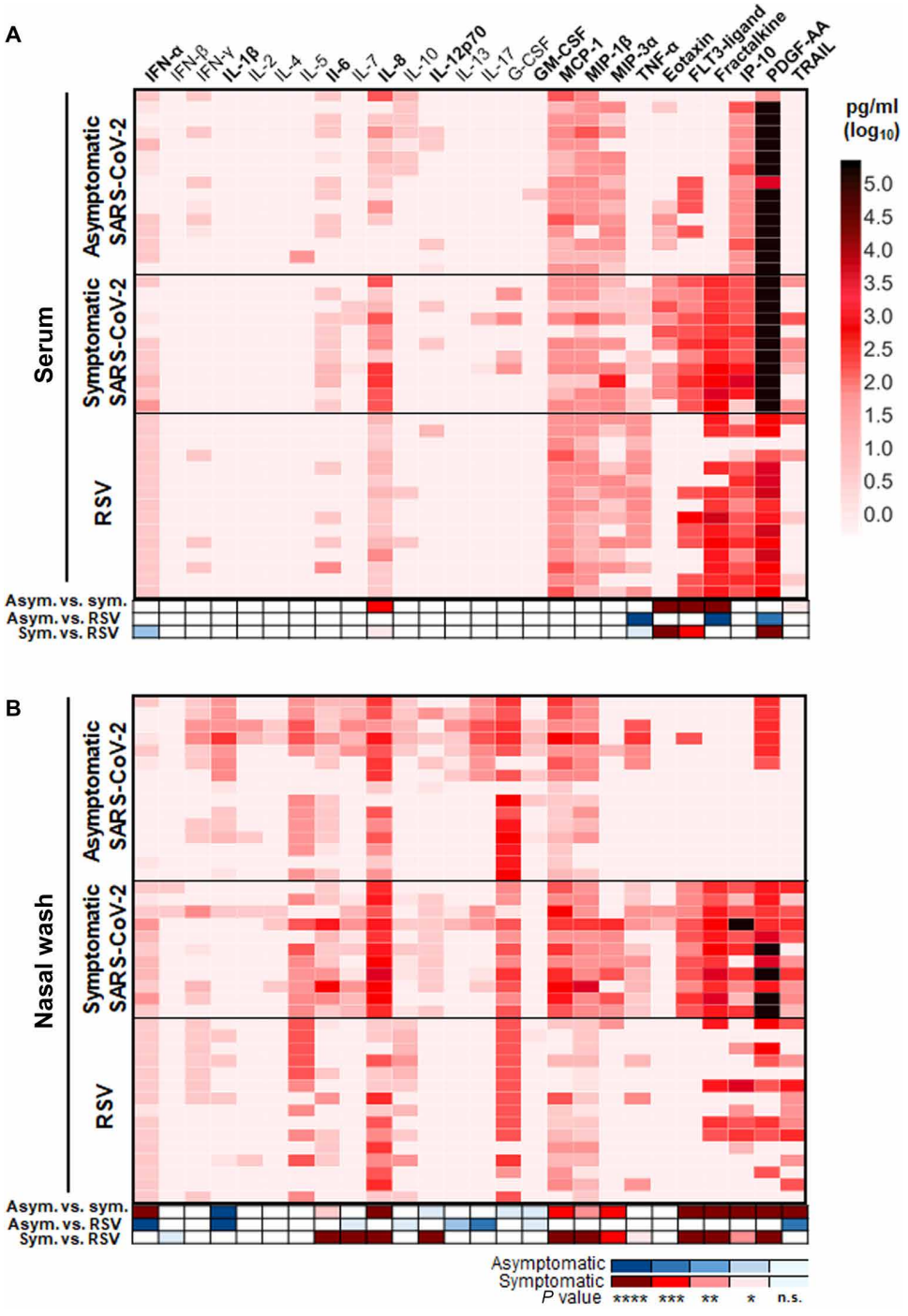

Fig. 1. Cytokine and chemokine profiles in sera and nasal washes from asymptomatic and symptomatic COVID-19 patients and RSV-infected adults. (**A** and **B**) Cytokine/chemokine profiling of serum samples versus nasal washes from SARS-CoV-2 and RSV-infected individuals. Heatmap of 26 cytokines/chemokines in SARS-CoV-2 asymptomatic (Asymp.) individuals ($n = 15$), SARS-CoV-2 symptomatic (Symp.) patients ($n = 11$), and symptomatic RSV-infected nonhospitalized normal males ($n = 15$). The color scale on the right represents concentration of each protein in picograms per milliliter. All serum/nasal wash samples were diluted fourfold and analyzed via a Bio-Plex Pro Human Cytokine Panel 17-Plex and R&D Systems individual human cytokine kits as per the manufacturer's instructions. The cytokine assay was performed in duplicate (two independent experiments by research fellow in the laboratory who was blinded to sample identity). Similar cytokine levels were observed in the two assays. Differences among groups were performed using R. The differences were considered statistically significant with a 95% confidence interval when the *P* value was less than 0.05 (*$P \leq 0.05$, **$P \leq 0.01$, ***$P \leq 0.001$, and ****$P \leq 0.0001$). Raw data are presented in tables S2 and S3. Additional comparisons between serum and nasal washes are shown in fig. S1. n.s., not significant.

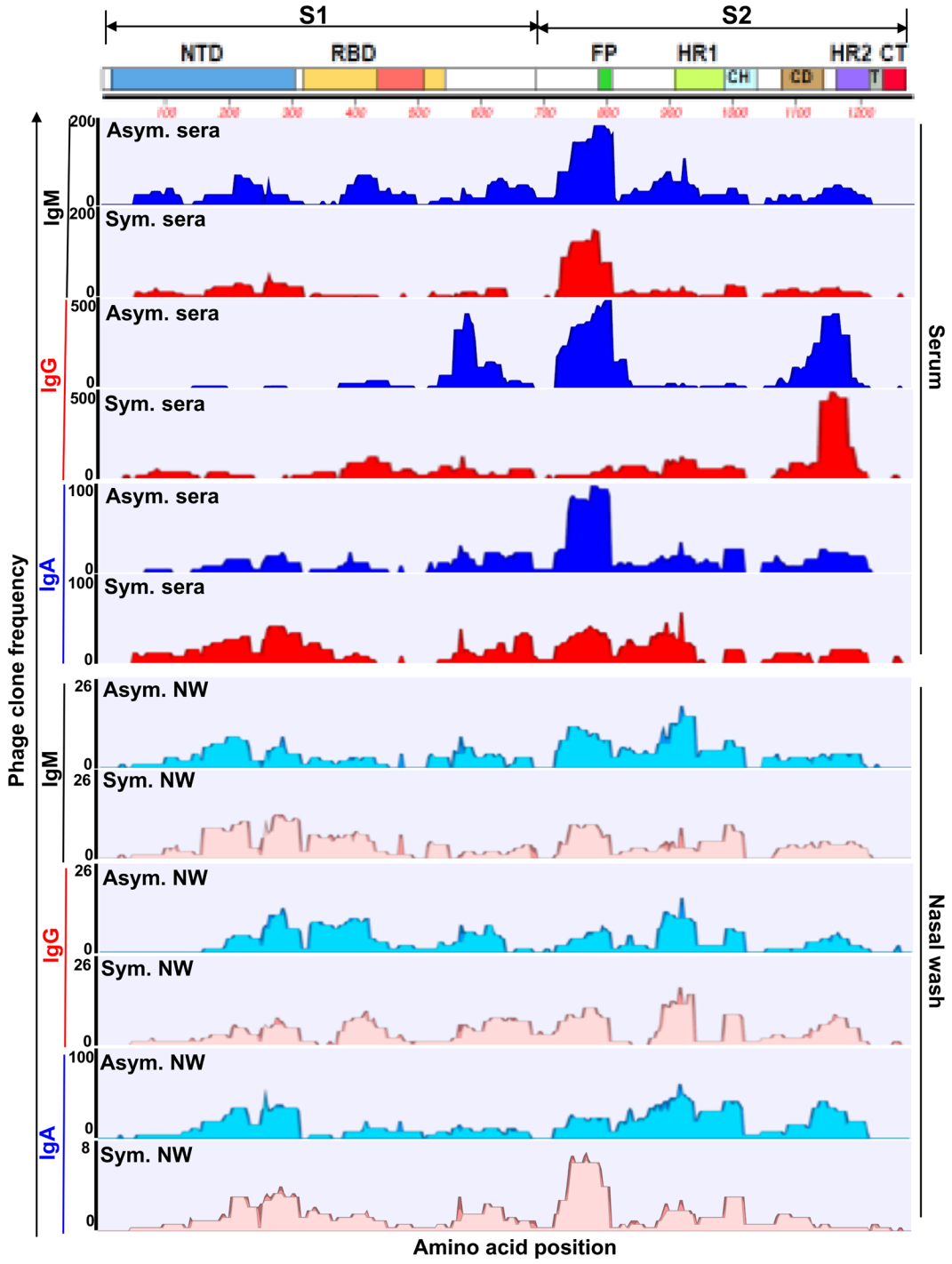

Fig. 2. SARS-CoV-2 antibody epitope repertoires recognized by serum and nasal wash antibodies of SARS-CoV-2–infected asymptomatic individuals versus symptomatic COVID-19 patients. IgM, IgG, and IgA antibody epitope repertoires recognized in sera and nasal washes from SARS-CoV-2–infected adults with asymptomatic or symptomatic infections, using SARS-CoV-2 spike GFPDL analysis. The schematic representation on top shows various domains in the SARS-CoV-2 spike. The raw data are shown in figs. S3 and S4. Epitope coverage map shows alignment position (amino acid position) on the *x* axis and coverage (phage clone frequency) of each position on the *y* axis defined by epitopes recognized by IgG, IgM, and IgA in asymptomatic patients' nasal wash (cyan) or serum (blue) versus symptomatic patients' nasal wash (pink) or serum (red), respectively. *y* axis is phage clone frequency in range of 0 to 200 for IgM, 0 to 500 for IgG, or 0 to 100 for IgA selections with serum. In nasal wash, the clone frequency ranges were 0 to 26 for IgM and IgG clones. IgA clones ranged from 0 to 100 for asymptomatic and from 0 to 8 for symptomatic patients. Samples were assayed fresh and not freeze-thawed. All samples were run in one batch at the same time for each assay. The GFPDL affinity selection was performed in duplicate (two independent experiments by research fellow in the laboratory, who was blinded to sample identity). Similar numbers of bound phage clones and epitope repertoire were observed in the two GFPDL panning. These data are further analyzed in figs. S3 to S6. NW, nasal wash.

the frequencies of antigenic sites bound by IgG and IgA in serum and nasal washes revealed some significant differences between asymptomatic and symptomatic SARS-CoV-2 patients that mapped to NTD, RBD, FP, and S2 domain (Fig. 2 and fig. S6). Some of these differential epitopes are shown on the trimeric structure of the spike in figs. S7 and S8 for nasal washes and serum samples, respectively. These findings suggest that serum-derived IgG and IgA antibodies can transudate into the mucosal spaces, but in addition, local B cell activation in the mucosal associated lymph nodes (especially IgA) contributes to the anti–SARS-CoV-2 spike responses as previously reported (*4*).

Serum and nasal wash antibody specificity against stabilized prefusion spike, RBD mutants, and neutralization of SARS-CoV-2 variants

To determine the spike and RBD-binding antibodies for individual pairs of serum and nasal washes, we performed SPR that allows for real-time kinetics measurements of antibody-antigen interactions. Furthermore, in our studies, the SARS-CoV-2 proteins were captured at a low density under conditions that ensure conformation integrity of the proteins (fig. S9), as previously described (*11*, *12*, *19*, *20*). Total antibody binding [resonance units (RU)] against the SARS-CoV-2–stabilized prefusion spike derived from the early circulating strain in the United States (WA-1) was measured for each of the matched serum/nasal wash pairs from the 15 SARS-CoV-2 asymptomatic adults, 11 acute symptomatic COVID-19 patients, and 15 RSV-infected adult controls (Fig. 3A). As expected, negligible anti–SARS-CoV-2 spike antibody reactivity was observed for either serum or nasal wash from the 15 symptomatic RSV-infected control samples (collected in 2015). Most of the asymptomatic and symptomatic SARS-CoV-2–infected adults had modest serum antibodies against the prefusion S with mean RU values of 106 and 70, respectively (Fig. 3A). In comparison with sera, the nasal washes from the same individuals showed lower RU values ranging from 6 to 100 (Fig. 3A). In light of the recently emerging VOCs around the world (*21*–*25*), we next measured binding of the paired serum and nasal washes to recombinant wild-type RBD domain derived from WA-1 (RBD-wt) and to two RBD mutants engineered to express key mutations in the South African (SA) variant, K417N (RBD-K417N) and E484K (RBD-E484K), that potentially affect antibody binding and virus neutralization (Fig. 3B). Antibody binding of sera from both asymptomatic and symptomatic SARS-Cov-2–infected individuals to the RBD-wt was robust in both groups, with significantly lower (4- to 10-fold) antibody binding for nasal washes. Total binding to RBD-K417N was very similar to the binding to RBD-wt for serum and nasal wash samples in both cohorts. In contrast, the binding of sera and nasal washes to the RBD-E484K was significantly reduced for both serum and nasal wash compared with RBD-wt (Fig. 3, B and C). Fold reduction of antibody binding to RBD-E484K mutant was higher in serum and nasal wash from symptomatic COVID-19 patients (3.45- and 2.81-fold, respectively) compared with reduction in binding in asymptomatic serum and nasal wash (2.1 and 1.91, respectively), but these differences did not reach statistical significance (Fig. 3C). These findings confirm the important role of amino acid E484K, located in the receptor binding motif, as target of antibodies, while K417N seems to play a minimal role in immune escape in both systemic and mucosal antibody response of symptomatic COVID-19 patients as well as asymptomatic SARS-CoV-2–infected adults.

In addition to measuring total antibody binding, the SPR real-time kinetics allowed us to compare the dissociation kinetics of antibody bound to the SARS-CoV-2 prefusion stabilized spike as a surrogate of antibody affinity. Slower antibody-antigen dissociation rates (off-rates) represent higher affinity antibodies. Unexpectedly, we observed that the affinity of prefusion spike bound antibodies in either sera or nasal washes from asymptomatic individuals were significantly higher than for sera and nasal washes from symptomatic SARS-CoV-2–infected individuals (Fig. 3D). Yet, in both groups, the affinity of nasal washes antibodies for the prefusion spike was ~5-fold lower than the paired serum samples (Fig. 3D).

Virus neutralization was measured against SARS-CoV-2 WA-1, UK VOC (B.1.1.7, Alpha), and SA VOC (B.1.351, Beta) strains using pseudovirus neutralization assay (PsVNA). Very broad range of neutralization titers was observed in the serum samples from either asymptomatic adults or symptomatic COVID-19 patients against the WA-1 strain (Fig. 3E). In these assays, no virus neutralization (titers < 20) was measured in nasal washes from either cohort (fig. S10). Mean twofold reduction in serum titers against the UK VOC (B.1.1.7) was observed in asymptomatic adults, while fourfold reduction was observed in mean serum titers of symptomatic COVID-19 patients (Fig. 3F). Greater reduction in serum neutralization titers was observed against the SA VOC (B.1.351), with mean 3.7-fold reduction for asymptomatic individuals with 100% seropositivity versus mean 9.3-fold reduction for symptomatic COVID-19 patients with seropositivity reduced to 73% (Fig. 3, E and F). These trends between asymptomatic versus symptomatic individuals within the SARS-COV-2 strain did not reach statistical significance.

DISCUSSION

Mucosal immunity (innate and adaptive) may play a key role in the early stages of upper respiratory tract infections contributing to control of the replicating virus after exposure and prevention of further virus spread to the bronchi and lower respiratory tract (*1*, *7*). Hence, efforts are under way to develop vaccines for mucosal delivery (*26*). Recent reports on mucosal versus systemic immunity focused on saliva samples (*2*, *3*) and one recent report on nasal fluids (*4*). However, there is limited knowledge on SARS-CoV-2 immune profile, especially antibody epitope diversity and antibody affinity at the mucosal sites, and their relation to serum immune response, especially in asymptomatic individuals who presumably control the viral infection in the upper respiratory tract.

In this study, we evaluated the systemic and mucosal immune signatures in asymptomatic adults versus symptomatic COVID-19 patients (10 days after PCR-confirmed infection). Paired serum/nasal washes were subjected to multiple analyses including epitope repertoire analyses using GFPDL, SPR-based antibody binding kinetics, PsVNA against wild-type strain (WA-1) and VOCs, and cytokine/chemokine analyses. The most important findings were (i) evidence for independent evolution of antibody responses in the mucosal sites as reflected in different ratios of IgM/IgG/IgA compared with serum and recognition of several unique epitopes across the spike (including S2); (ii) the cytokine/chemokine responses demonstrated differential patterns in nasal washes of symptomatic compared with asymptomatic individuals. Elevated IL-1β and G-CSF were observed in nasal washes of asymptomatic individuals, while higher IL-6, IL-8, IFN-α, TRAIL, and multiple chemokines were found in symptomatic COVID-19 patients; (iii) affinity of antibodies against

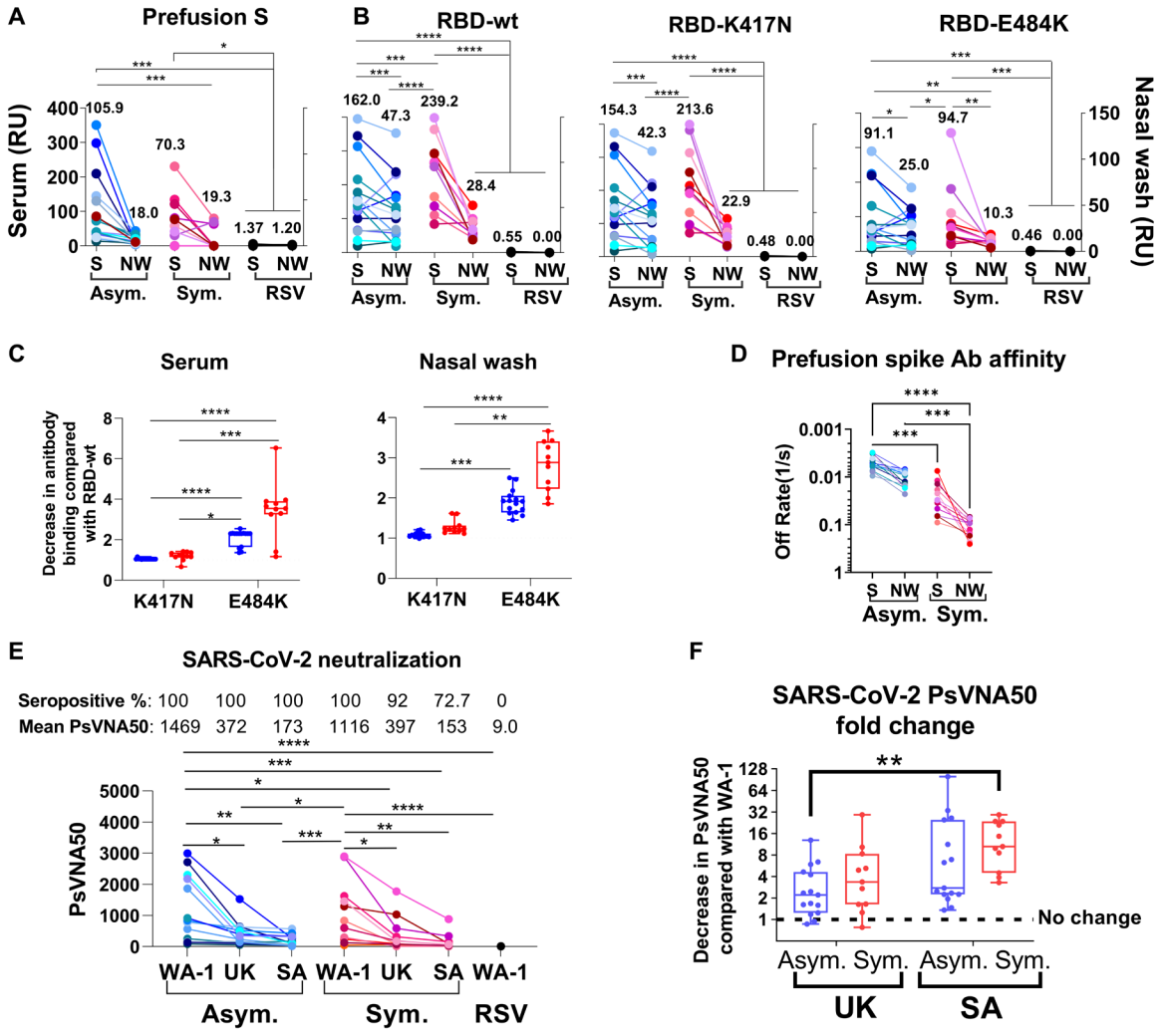

Fig. 3. Serum versus mucosal antibody binding kinetics and neutralization of SARS-CoV-2 variants in sera and nasal washes from asymptomatic and symptomatic COVID-19 patients. (**A** and **B**) SPR-based antibody binding [maximum resonance units (RU)] of serum (S) and nasal wash (NW) pairs to purified SARS-CoV-2 prefusion spike (A), and RBD-wt and mutants RBD-K417N and RBD-E484K (B). Total antibody binding of 10-fold diluted samples from SARS-CoV-2 asymptomatic (n = 15, blue), symptomatic COVID-19 (n = 11, red), and symptomatic RSV-infected nonhospitalized (n = 15, black) individuals. Mean values for each group are shown above. (**C**) Fold decrease in antibody binding to mutants RBD-K417N and RBD-E484K of serum or nasal wash from asymptomatic (blue) or symptomatic (red) COVID-19 patients. (**D**) Antibody (Ab) affinity of serum and nasal wash pairs from asymptomatic (n = 15, blue) versus symptomatic COVID-19 individuals (n = 11, red) to prefusion spike. (**E**) PsVNA50 titers of serum and nasal wash of asymptomatic (n = 15, blue), symptomatic COVID-19 (n = 11, red), and symptomatic RSV-infected nonhospitalized (n = 15, black) individuals against WA-1, UK, and SA strains. (**F**) Fold decrease in serum PsVNA50 against UK and SA in comparison with WA-1 strain. Statistical differences between the groups were determined using R and considered significant when the P value was less than 0.05 (*$P \leq 0.05$, **$P \leq 0.01$, ***$P \leq 0.001$, and ****$P \leq 0.0001$). The data shown are average values of two experimental runs.

the prefusion stabilized spike protein was significantly higher in serum and nasal washes of asymptomatic individuals compared with symptomatic COVID-19 patients; and (iv) differential serum neutralization activity against WA-1 compared with the UK (Alpha) and SA (Beta) VOCs in both asymptomatic and symptomatic individuals.

In addition to paired samples from COVID-19 patients, we analyzed serum and nasal washes from symptomatic RSV-infected but nonhospitalized normal adults (matched for sex and age with the COVID-19 patients). Because many of the early innate response biomarkers in the upper respiratory tract are likely to be shared among respiratory viral infections, it is important to include such a disease comparator group to fully decipher the common versus pathogen-specific cytokine/chemokine patterns following SARS-CoV-2 infection. The extent of local cytokine/chemokine response in the nasal washes suggested a robust local innate response to infection that was somewhat different between asymptomatic versus symptomatic SARS-CoV-2–infected individuals, especially the levels of chemokines including eotaxin, FLT3 ligand, fractalkine, PDGF-AA, and TRAIL were greatly elevated in the nasal washes from symptomatic COVID-19 patients. These mediators are strong attractants for monocytes and neutrophils and also involved in cellular apoptosis. Virus replication most likely trigger multiple innate cells that line the mucosal surfaces, and the chemokines attract inflammatory macrophages and neutrophils. IL-1β and G-CSF secretion was higher in asymptomatic versus symptomatic individuals,

while higher levels of IL-6, IL-8, and IFN-α were observed in nasal washes of symptomatic COVID-19 patients. The pattern of mucosal cytokine/chemokines in the nasal wash of symptomatic COVID-19 patients was similar to those observed in the nasal washes of the symptomatic RSV adult patients, suggesting a common mechanism of local innate responses to replicating viruses in the URT. The levels of antiviral and proinflammatory cytokines and chemokines can determine the balance between virus control versus tissue damage that takes place in the nasal cavity with eventual spillover to the lower respiratory tract and the blood. Pierce *et al.* (*7*) recently described a more vigorous early activation of innate immune pathways in the nasopharynx of children compared with adults, including higher levels of IFN-α2, IFN-γ, IP10, IL-8, and IL-1β, at clinical presentation with COVID-19, which inversely correlated with disease severity.

In the GFPDL, IgA-bound phages in nasal washes were 100-fold higher in asymptomatic individuals compared with symptomatic patients, probably indicative of an important role for mucosal IgA in early protection against the virus as previously suggested (*4*, *27*, *28*). It is expected that most of the mucosal IgA in the nasal washes was secretory IgA, which can form dimers and oligomers that can bind virions and may help in viral clearance (*29*). The GFPDL analyses identified several antigenic sites that were more frequently recognized by nasal wash (IgA and IgG) antibodies compared with the serum antibodies (figs. S6 to S8). Among those, recognition of antigenic sites encompassing 260 to 331, 418 to 510, 548 to 590, 789 to 873 (containing FP), 883 to 964, 944 to 1001, and 1115 to 1181 was more common in nasal wash IgA/IgG of asymptomatic compared with symptomatic COVID-19 individuals. This finding requires follow-up in future evaluation of SARS-CoV-2 infections, including measurements of virus shedding, that may provide immune correlates of protection not only from severe diseases but also from transmission to secondary hosts. One of the possible limitations of GFPDL-based assessments is that while the phage display is likely to detect both conformational and linear epitopes on the SARS-CoV-2 spike protein, they are unlikely to detect paratopic interactions that may require posttranslational modifications or quaternary epitopes formed by cross-protomers. In addition, because limited volumes of matched serum/nasal wash pairs available from these SARS-CoV-2–infected individuals, elucidation of antibody epitope repertoire using phage display library was performed on pooled sera samples to get a more "global" signature of antibody repertoire generated following SARS-CoV-2 infection rather than to characterize antibody response in each individual. Recently, we performed spike gene–based GFPDL analysis on pooled versus individual serum samples in older COVID-19 adults (60 to 70 years of age) (*12*, *16*). This GFPDL analyses demonstrated that IgG, IgM, or IgA spike antibody epitope repertoire in individual sera was similar to that identified with pooled sera, suggesting that GFPDL data observed with pooled sera are a meaningful representation of overall antibody profile in individuals.

Because several intranasal SARS-CoV-2 vaccines and therapeutics are in early clinical trials (including live attenuated vaccine), it will be important to compare the epitope profiles after vaccination versus after infection in the mucosal sites and explore their correlation with control of virus replication and progression to severe disease.

In SPR, total antibody binding of nasal washes was 5- to 10-fold lower than for serum samples. The E484K mutation affected antibody binding to the RBD significantly, while the K417N had minimal impact. These findings are in agreement with other studies on the contribution of different amino acid mutations in the B.1.351 to loss of antibody binding (*30*). In our study, virus neutralization titers were minimal or undetectable in nasal washes despite weak/moderate antibody binding to the SARS-CoV-2 prefusion spike and RBD. Other studies on mucosal antibodies in nasal washes also described only spike-binding antibodies (but not neutralizing antibodies following infection) (*4*, *7*). It is unclear whether this reflects timing of sampling (early after infection) or the presence of unidentified inhibitors in mucosal fluid that interfere with the neutralization assays. On the other hand, nonneutralizing antibodies may also contribute to virus clearance via Fc-mediated functions like phagocytosis or complement fixation, as previously reported in COVID-19 patients (*31*, *32*).

Antibody affinity plays a key role in protective immunity and was shown to correlate with control of viral loads after avian influenza infections in ferrets (*33*–*35*) and improved clinical outcome in Zika, Ebola, and influenza patients (*20*, *36*, *37*). After SARS-CoV-2 infection, antibody affinity maturation occurs gradually over several months (*38*, *39*). On the other hand, we recently observed that antibody affinity maturation is blunted in severe hospitalized COVID-19 patients that did succumbed to the disease compared with surviving patients (*12*, *40*) and antibody affinity maturation correlated with lower disease severity in hospitalized COVID-19 patients (*16*). In the current study, we found five- to eightfold lower serum antibody affinity against the SARS-CoV-2 prefusion spike in symptomatic hospitalized COVID-19 patients compared with asymptomatic individuals. A similar difference in antibody affinity was also found for nasal wash antibodies in the two cohorts. Evidence for blunted germinal center (GC) formation in lymph nodes from severe COVID-19 patients associated with reduced Bcl-6 expressing T follicular helper cells (Tfh) was recently described by Kaneko *et al.* (*41*). However, in our earlier studies, antibody affinity was found to be significantly higher in patients who survived compared with deceased individuals (*12*). Here, we measured higher affinity antibodies in asymptomatic individuals in both serum and nasal wash compared with symptomatic COVID-19 patients (including two patients who required mechanical ventilation) at 10 days after PCR-confirmed SARS-CoV-2 infections. Thus, antibody evolution including class switching and affinity maturation may take place early after infection in lymph nodes across the body including those associated with the upper and lower respiratory tract. Local virus replication in the upper respiratory tract is likely to be a strong driver of GC formation in the mucosal-associated lymph nodes, and affinity maturation of plasma cells can subsequently spread systemically. The underlining mechanisms of reduced GC development in more severe COVID-19 require further investigation. The specificity, affinity, and functions of mucosal antibodies are likely to affect virus replication, disease progression, and transmission.

The limitation of our study was the relatively small size of our cohorts that only included males. Hence, these study observations interpretation may not be commutable to females. It will be important to include individuals of both sexes in subsequent studies and to follow patients for longer time through convalescence. Durability of mucosal immunity may predict the rate of reinfections following recovery from primary infection and following vaccination.

Together, our data suggest that studies performed with systemic immune responses may not fully reflect the innate and adaptive

immune responses at the mucosal sites in the upper respiratory tract, which play a critical role in early virus control, underscoring the importance of localized immune responses including IgG/IgA class switching and antibody affinity following SARS-CoV-2 infection.

In summary, elucidating the quality of immune response in SARS-CoV-2–infected individuals at the site of infection in comparison with the systemic response could be highly beneficial for understanding the host immune response and could guide effective intervention strategies and rational development of targeted vaccines and therapeutics against SARS-CoV-2.

METHODS

Study design

Study samples were purchased from Antibody Systems Inc. Matched serum and nasal wash pairs were obtained from 15 asymptomatic SARS-CoV-2–infected males in Florida. The paired samples were collected at 10 days after confirmed positive SARS-CoV-2 reverse transcription PCR (RT-PCR) test from adult males (table S1). All males were asymptomatic. Age-matched and time-matched serum-nasal wash pairs were obtained from 11 symptomatic SARS-CoV-2–infected males at 10 days after confirmed positive SARS-CoV-2 RT-PCR test who became symptomatic after positive PCR test and were hospitalized. All symptomatic patients were hospitalized because of COVID-19. Two hospitalized COVID-19 patients required mechanical ventilation. All hospitalized COVID-19 patients recovered from disease and were released from the hospital. Age-matched (age ranging from 21 to 57 years) control serum-nasal wash pairs from symptomatic RSV-infected nonhospitalized normal males were obtained in 2015 (table S1). Serum and respiratory samples were tested for SARS-CoV-2 infection by SARS-CoV-2 by PCR or RT–quantitative PCR using the Thermo Fisher Scientific SARS-CoV-2 RT-PCR Kit. Demographic, clinical, and outcome data for each individual is provided in table S1. Deidentified samples were tested in different antibody assays under exempt status approval from the U.S. Food and Drug Administration's Research Involving Human Subjects Committee [FDA-RIHSC-2020-04-02 (252)]. Samples and assays were run in duplicate or triplicate. Research fellows running the antibody assays were blinded to the identity of the groups for assessments of outcomes.

Proteins

The SARS-CoV-2 spike plasmid expressing genetically stabilized prefusion 2019-nCoV_S-2P spike ectodomain, a gene encoding residues 1 to 1208 of 2019-nCoV S fused to 8xHisTag was a gift from B. Graham (Vaccine Research Center, National Institutes of Health) (*42*). This expression vector was used to transiently transfect Free Style 293F cells (Thermo Fisher Scientific) using polyethyleneimine. Protein was purified from filtered cell supernatants using StrepTactin resin and subjected to additional purification by size exclusion chromatography in phosphate-buffered saline (PBS). Recombinant SARS-CoV-2 spike RBD and its mutants were purchased from Sino Biologicals (RBD-wt, 40592-V08H82; RBD-K417N, 40592-V08H59; and RBD-E484K, 40592-V08H84). Recombinant purified proteins used in the study were produced in 293 mammalian cells (prefusion spike and RBDs). The native receptor-binding activity of the spike proteins was determined by binding to the human angiotensin converting enzyme 2 (ACE2) protein (5 μg/ml) (*11*, *12*, *16*).

Measurement of cytokine levels in serum and nasal wash

All serum/nasal wash samples were diluted fourfold in Bio-Plex Sample Diluent HB buffer. The samples were analyzed via a Bio-Plex Pro Human Cytokine Panel 17-Plex assay as per the manufacturer's instructions. Plates were read using the Bio-Plex 200 system (Bio-Rad, Hercules, CA). Additional nine cytokines included measurement of type 1 IFN were determined using the individual human cytokine kits (R&D Systems, Minneapolis, MN). The cytokine assay was performed in duplicate (two independent experiments by research fellow in the laboratory who was blinded to sample identity). Similar cytokine levels were observed in the two assays.

SARS-CoV-2 pseudovirus production and neutralization assay

Pseudovirion production and PsVNA were described in previous publications from our laboratory (*11*, *12*, *16*). Briefly, human codon-optimized cDNA encoding SARS-CoV-2 S glycoprotein of the WA-1 strain, UK variant (B.1.1.7 with spike mutations: H69-V70del, Y144del, N501Y, A570D, D614G, P681H, T716I, S982A, and D1118H), and SA variant (B.1.351 strain with spike mutations L18F, D80A, D215G, L242-244del, R246I, K417N, E484K, N501Y, D614G, and A701V) was synthesized by GenScript and cloned into eukaryotic cell expression vector pcDNA 3.1 between the Bam HI and Xho I sites. Pseudovirions were produced by cotransfection Lenti-X 293 T cells with psPAX2(gag/pol), pTrip-luc lentiviral vector, and pcDNA 3.1 SARS-CoV-2–spike–deltaC19 using Lipofectamine 3000. The supernatants were harvested at 48 hours after transfection and filtered through 0.45-μm membranes and titrated using 293 T-ACE2 cells (human embryonic kidney–293T cells that express ACE2 protein, as described previously (*43*).

For the neutralization assay, 50 μl of SARS-CoV-2 S pseudovirions was preincubated with an equal volume of medium containing serum at varying dilutions at room temperature for 1 hour, and then virus-antibody mixtures were added to 293 T-ACE2 cells in a 96-well plate. After a 3-hour incubation, the inoculum was replaced with fresh medium. Cells were lysed 24 hours later, and luciferase activity was measured using luciferin. Controls included cell only control, virus without any antibody control, and positive control sera. The cutoff value or the limit of detection for neutralization assay is 1:10. The PsVNA was performed twice, and the researchers performing the assay were blinded to sample identity.

SARS-CoV-2 GFPDL construction

SARS-CoV-2 spike GFPDL construction was described in previous publications from our laboratory (*11*, *12*, *16*). Briefly, DNA encoding the spike gene of SARS-CoV-2 isolate Wuhan-Hu-1 strain (GenBank, MN908947.3) was chemically synthesized and used for cloning. A gIII display-based phage vector, fSK-9-3, was used where the desired polypeptide can be displayed on the surface of the phage as a gIII-fusion protein. Purified DNA containing spike gene was digested with deoxyribonuclease I to obtain gene fragments of 50– to 1500–base pair size range (18 to 500 amino acids) and used for GFPDL construction, as described previously (*11*, *12*, *16*).

Affinity selection of SARS-CoV-2 GFPDL phages with polyclonal human serum/nasal wash

SARS-CoV-2 GFPDL-based affinity selection was performed as described before (*11*, *12*, *16*). Briefly, equal volumes of each of the human serum/nasal wash from 15 asymptomatic individuals or

RSV-infected adults or 11 symptomatic COVID-19 patients were used for GFPDL panning. Before panning of GFPDL with polyclonal serum/nasal wash antibodies, serum/nasal wash components, which could nonspecifically interact with phage proteins, were removed by incubation with ultraviolet-killed M13K07 phage-coated petri dishes. GFPDL affinity selection was carried out in-solution with anti-IgM, protein A/G (IgG), or anti-IgA specific affinity resin.

The pooled serum/nasal wash was incubated with the GFPDL and the specific resin, and the unbound phages were removed by PBST (PBS containing 0.1% Tween 20) wash followed by PBS. Bound phages were eluted by addition of 0.1 N of Gly-HCl (pH 2.2) and neutralized by adding 8 μl of 2 M tris solution per 100 μl of eluate. After panning, antibody-bound phage clones were amplified, the inserts were sequenced, and the sequences were aligned to the SARS-CoV-2 spike gene to define the fine epitope specificity in these polyclonal samples.

The GFPDL affinity selection was performed in duplicate (two independent experiments by research fellow in the laboratory who was blinded to sample identity). Similar numbers of bound phage clones and epitope repertoire were observed in the two GFPDL panning.

Adsorption of polyclonal human postinfection serum on SARS-CoV-2 GFPDL phages and residual reactivity to SARS-CoV-2 prefusion spike

Adsorption using SARS-CoV-2 spike GFPDL construction was described previously (*11*, *12*, *16*). Briefly, before panning of GFPDL, serum and nasal wash antibodies from SARS-CoV-2–confirmed individuals were adsorbed by incubation with SARS-CoV-2 GFPDL phage-coated petri dishes. To ascertain the residual antibodies specificity, an ELISA was performed with wells coated with purified recombinant SARS-CoV-2 prefusion spike (100 ng/100 μl). After blocking with PBST containing 2% bovine serum albumin (BSA), serial dilutions of human serum (with or without GFPDL adsorption) in blocking solution were added to each well, incubated for 1 hour at room temperature, followed by addition of 5000-fold diluted horseradish peroxidase–conjugated goat anti-human IgA-IgG-IgM–specific antibody, and developed by 100 μl of o-phenylenediamine dihydrochloride (OPD) substrate solution. Absorbance was measured at 490 nm.

Antibody binding kinetics of post–SARS-CoV-2 infection human serum/nasal wash to recombinant SARS-CoV-2 proteins by SPR

SARS-CoV-2 antibody binding kinetics by SPR was described in previous publications from our laboratory (*11*, *12*, *16*, *19*). Briefly, steady-state equilibrium binding of post–SARS-CoV-2–infected human polyclonal samples was monitored at 25°C using a ProteOn SPR (Bio-Rad). The purified recombinant SARS-CoV-2 proteins were captured to a Ni-NTA sensor chip with 200 RU in the test flow channels. The protein density on the chip was optimized such as to measure monovalent interactions independent of the antibody isotype (*11*, *12*, *16*, *19*).

Serial dilutions (10-, 50-, and 250-fold) of freshly prepared serum/nasal wash in BSA-PBST buffer [PBS (pH 7.4) buffer with Tween 20 and 2% BSA] were injected at a flow rate of 50 μl/min (120-s contact duration) for association, and disassociation was performed over a 600-s interval. Responses from the protein surface were corrected for the response from a mock surface and for responses from a buffer-only injection. SPR was performed with serially diluted serum/nasal wash of each individual time point in this study. Total antibody binding and antibody isotype analysis were calculated with Bio-Rad ProteOn manager software (version 3.1). All SPR experiments were performed twice, and the researchers performing the assay were blinded to sample identity. In these optimized SPR conditions, the variation for each sample in duplicate SPR runs was <5%. The maximum RU data shown in the figures were the calculated RU signal for the 10-fold diluted serum/nasal wash sample.

Statistical analysis

All experimental data to compare differences between groups were analyzed using lme4 and emmeans packages in R (RStudio version 1.1.463). Data from cytokine, antibody binding, or neutralization analysis (used as independent variables) were analyzed for statistical significance for serum and nasal wash among various groups (asymptomatic versus symptomatic versus RSV) and controlled for "age" that served as a covariate (predictor variable) using a linear regression model. To ensure robustness of the results, absolute measurements were $\log_2$-transformed before performing the analysis. For each cytokine, antibody binding or neutralization data, the respective measurement was regressed on age and the various groups (factor variables). The tests were two-sided tests. For comparisons between the various groups, pairwise comparisons were extracted using "emmeans" and Tukey-adjusted P values were used for denoting significance to reduce type 1 error due to multiple testing. The differences were considered statistically significant with a 95% confidence interval when the P value was less than 0.05 ($^*P < 0.05$, $^{**}P < 0.01$, $^{***}P < 0.001$, and $^{****}P < 0.0001$).

SUPPLEMENTARY MATERIALS

Supplementary material for this article is available at https://science.org/doi/10.1126/sciadv.abi6533

View/request a protocol for this paper from *Bio-protocol*.

REFERENCES AND NOTES

1. Y. X. Chao, O. Rotzschke, E. K. Tan, The role of IgA in COVID-19. *Brain Behav. Immun.* **87**, 182–183 (2020).
2. B. Isho, K. T. Abe, M. Zuo, A. J. Jamal, B. Rathod, J. H. Wang, Z. Li, G. Chao, O. L. Rojas, Y. M. Bang, A. Pu, N. Christie-Holmes, C. Gervais, D. Ceccarelli, P. Samavarchi-Tehrani, F. Guvenc, P. Budylowski, A. Li, A. Paterson, Y. F. Yun, L. M. Marin, L. Caldwell, J. L. Wrana, K. Colwill, F. Sicheri, S. Mubareka, S. D. Gray-Owen, S. J. Drews, W. L. Siqueira, M. Barrios-Rodiles, M. Ostrowski, J. M. Rini, Y. Durocher, A. J. McGeer, J. L. Gommerman, A. C. Gingras, Persistence of serum and saliva antibody responses to SARS-CoV-2 spike antigens in COVID-19 patients. *Sci. Immunol.* **5**, eabe5511 (2020).
3. A. Varadhachary, D. Chatterjee, J. Garza, R. P. Garr, C. Foley, A. Letkeman, J. Dean, D. Haug, J. Breeze, R. Traylor, A. Malek, R. Nath, L. Linbeck III, Salivary anti-SARS-CoV-2 IgA as an accessible biomarker of mucosal immunity against COVID-19. *medRxiv*, (2020).
4. C. Cervia, J. Nilsson, Y. Zurbuchen, A. Valaperti, J. Schreiner, A. Wolfensberger, M. E. Raeber, S. Adamo, S. Weigang, M. Emmenegger, S. Hasler, P. P. Bosshard, E. De Cecco, E. Bächli, A. Rudiger, M. Stüssi-Helbling, L. C. Huber, A. S. Zinkernagel, D. J. Schaer, A. Aguzzi, G. Kochs, U. Held, E. Probst-Müller, S. K. Rampini, O. Boyman, Systemic and mucosal antibody responses specific to SARS-CoV-2 during mild versus severe COVID-19. *J. Allergy Clin. Immunol.* **147**, 545–557.e9 (2021).
5. R. Wölfel, V. M. Corman, W. Guggemos, M. Seilmaier, S. Zange, M. A. Müller, D. Niemeyer, T. C. Jones, P. Vollmar, C. Rothe, M. Hoelscher, T. Bleicker, S. Brünink, J. Schneider, R. Ehmann, K. Zwirglmaier, C. Drosten, C. Wendtner, Virological assessment of hospitalized patients with COVID-2019. *Nature* **581**, 465–469 (2020).
6. J. E. Bryant, A. S. Azman, M. J. Ferrari, B. F. Arnold, M. F. Boni, Y. Boum, K. Hayford, F. J. Luquero, M. J. Mina, I. Rodriguez-Barraquer, J. T. Wu, D. Wade, G. Vernet, D. T. Leung, Serology for SARS-CoV-2: Apprehensions, opportunities, and the path forward. *Sci. Immunol.* **5**, eabc6347 (2020).
7. C. A. Pierce, S. Sy, B. Galen, D. Y. Goldstein, E. Orner, M. J. Keller, K. C. Herold, B. C. Herold, Natural mucosal barriers and COVID-19 in children. *JCI Insight* **6**, (2021).

8. S. Khurana, A. L. Suguitan, Y. Rivera, C. P. Simmons, A. Lanzavecchia, F. Sallusto, J. Manischewitz, L. R. King, K. Subbarao, H. Golding, Antigenic fingerprinting of H5N1 avian influenza using convalescent sera and monoclonal antibodies reveals potential vaccine and diagnostic targets. *PLoS Med.* **6**, e1000049 (2009).
9. S. Fuentes, E. M. Coyle, J. Beeler, H. Golding, S. Khurana, Antigenic fingerprinting following primary RSV Infection in young children identifies novel antigenic sites and reveals unlinked evolution of human antibody repertoires to fusion and attachment glycoproteins. *PLOS Pathog.* **12**, e1005554 (2016).
10. S. Khurana, E. M. Coyle, J. Manischewitz, L. R. King, J. Gao, R. N. Germain, P. L. Schwartzberg, J. S. Tsang, H. Golding; CHI Consortium, AS03-adjuvanted H5N1 vaccine promotes antibody diversity and affinity maturation, NAI titers, cross-clade H5N1 neutralization, but not H1N1 cross-subtype neutralization. *NPJ Vaccines* **3**, 40 (2018).
11. S. Ravichandran, E. M. Coyle, L. Klenow, J. Tang, G. Grubbs, S. Liu, T. Wang, H. Golding, S. Khurana, Antibody signature induced by SARS-CoV-2 spike protein immunogens in rabbits. *Sci. Transl. Med.* **12**, eabc3539 (2020).
12. J. Tang, S. Ravichandran, Y. Lee, G. Grubbs, E. M. Coyle, L. Klenow, H. Genser, H. Golding, S. Khurana, Antibody affinity maturation and plasma IgA associate with clinical outcome in hospitalized COVID-19 patients. *Nat. Commun.* **12**, 1221 (2021).
13. S. Fuentes, M. Hahn, K. Chilcote, R. F. Chemaly, D. P. Shah, X. Ye, V. Avadhanula, P. A. Piedra, H. Golding, S. Khurana, Antigenic fingerprinting of Respiratory Syncytial Virus (RSV)-a-infected hematopoietic cell transplant recipients reveals importance of mucosal anti-RSV G antibodies in control of RSV infection in humans. *J. Infect. Dis.* **221**, 636–646 (2020).
14. N. Mangalmurti, C. A. Hunter, Cytokine storms: Understanding COVID-19. *Immunity* **53**, 19–25 (2020).
15. L. A. Pirofski, A. Casadevall, Pathogenesis of COVID-19 from the Perspective of the Damage-Response Framework. *MBio* **11**, 4 (2020).
16. S. Ravichandran, Y. Lee, G. Grubbs, E. M. Coyle, L. Klenow, O. Akasaka, M. Koga, E. Adachi, M. Saito, I. Nakachi, T. Ogura, R. Baba, M. Ito, M. Kiso, A. Yasuhara, S. Yamada, Y. Sakai-Tagawa, K. Iwatsuki-Horimoto, M. Imai, S. Yamayoshi, H. Yotsuyanagi, Y. Kawaoka, S. Khurana, Longitudinal antibody repertoire in "mild" versus "severe" COVID-19 patients reveals immune markers associated with disease severity and resolution. *Sci. Adv.* **7**, eabf2467 (2021).
17. E. Shrock, E. Fujimura, T. Kula, R. T. Timms, I. H. Lee, Y. Leng, M. L. Robinson, B. M. Sie, M. Z. Li, Y. Chen, J. Logue, A. Zuiani, D. McCulloch, F. J. N. Lelis, S. Henson, D. R. Monaco, M. Travers, S. Habibi, W. A. Clarke, P. Caturegli, O. Laeyendecker, A. Piechocka-Trocha, J. Z. Li, A. Khatri, H. Y. Chu; MGH COVID-19 Collection & Processing Team16‡, A. C. Villani, K. Kays, M. B. Goldberg, N. Hacohen, M. R. Filbin, X. G. Yu, B. D. Walker, D. R. Wesemann, H. B. Larman, J. A. Lederer, S. J. Elledge, Viral epitope profiling of COVID-19 patients reveals cross-reactivity and correlates of severity. *Science* **370**, eabd4250 (2020).
18. M. Dugas, T. Grote-Westrick, R. Vollenberg, E. Lorentzen, T. Brix, H. Schmidt, P. R. Tepasse, J. Kühn, Less severe course of COVID-19 is associated with elevated levels of antibodies against seasonal human coronaviruses OC43 and HKU1 (HCoV OC43, HCoV HKU1). *Int. J. Infect. Dis.* **105**, 304–306 (2021).
19. S. Khurana, M. Hahn, E. M. Coyle, L. R. King, T. L. Lin, J. Treanor, A. Sant, H. Golding, Repeat vaccination reduces antibody affinity maturation across different influenza vaccine platforms in humans. *Nat. Commun.* **10**, 3338 (2019).
20. S. Khurana, S. Ravichandran, M. Hahn, E. M. Coyle, S. W. Stonier, S. E. Zak, J. Kindrachuk, R. T. Davey Jr., J. M. Dye, D. S. Chertow, Longitudinal human antibody repertoire against complete viral proteome from ebola virus survivor reveals protective sites for vaccine design. *Cell Host Microbe* **27**, 262–276.e4 (2020).
21. D. M. Altmann, R. J. Boyton, R. Beale, Immunity to SARS-CoV-2 variants of concern. *Science* **371**, 1103–1104 (2021).
22. L. A. Dos Santos, P. G. de Góis Filho, A. M. F. Silva, J. V. G. Santos, D. S. Santos, M. M. Aquino, R. M. de Jesus, M. L. D. Almeida, J. S. da Silva, D. M. Altmann, R. J. Boyton, C. A. D. Santos, C. N. O. Santos, J. C. Alves, I. L. Santos, L. S. Magalhães, E. M. M. A. Belitardo, D. J. P. G. Rocha, J. P. P. Almeida, L. G. C. Pacheco, E. R. G. R. Aguiar, G. S. Campos, S. I. Sardi, R. H. Carvalho, A. R. de Jesus, K. F. Rezende, R. P. de Almeida, Recurrent COVID-19 including evidence of reinfection and enhanced severity in thirty Brazilian healthcare workers. *J. Inf. Secur.* **82**, 399–406 (2021).
23. K. Kupferschmidt, Fast-spreading U.K. virus variant raises alarms. *Science* **371**, 9–10 (2021).
24. K. Kupferschmidt, New mutations raise specter of 'immune escape'. *Science* **371**, 329–330 (2021).
25. C. K. Wibmer, F. Ayres, T. Hermanus, M. Madzivhandila, P. Kgagudi, B. Oosthuysen, B. E. Lambson, T. de Oliveira, M. Vermeulen, K. van der Berg, T. Rossouw, M. Boswell, V. Ueckermann, S. Meiring, A. von Gottberg, C. Cohen, L. Morris, J. N. Bhiman, P. L. Moore, SARS-CoV-2 501Y.V2 escapes neutralization by South African COVID-19 donor plasma. *Nat. Med.* **27**, 622–625 (2021).
26. P. de Sousa-Pereira, J. M. Woof, IgA: Structure, function, and developability. *Antibodies* **8**, 57 (2019).
27. J. Dan, S. Mehta, SARS-CoV-2 immunity and reinfection. *Clin. Infect. Dis.* **2021**, ciaa1936 (2021).
28. Z. Wang, J. C. C. Lorenzi, F. Muecksch, S. Finkin, C. Viant, C. Gaebler, M. Cipolla, H. H. Hoffmann, T. Y. Oliveira, D. A. Oren, V. Ramos, L. Nogueira, E. Michailidis, D. F. Robbiani, A. Gazumyan, C. M. Rice, T. Hatziioannou, P. D. Bieniasz, M. Caskey, M. C. Nussenzweig, Enhanced SARS-CoV-2 neutralization by dimeric IgA. *Sci. Transl. Med.* **13**, eabf1555 (2021).
29. N. Kumar, C. P. Arthur, C. Ciferri, M. L. Matsumoto, Structure of the secretory immunoglobulin A core. *Science* **367**, 1008–1014 (2020).
30. P. Wang, M. S. Nair, L. Liu, S. Iketani, Y. Luo, Y. Guo, M. Wang, J. Yu, B. Zhang, P. D. Kwong, B. S. Graham, J. R. Mascola, J. Y. Chang, M. T. Yin, M. Sobieszczyk, C. A. Kyratsous, L. Shapiro, Z. Sheng, Y. Huang, D. D. Ho, Antibody resistance of SARS-CoV-2 variants B.1.351 and B.1.1.7. *Nature* **593**, 130–135 (2021).
31. T. Zohar, G. Alter, Dissecting antibody-mediated protection against SARS-CoV-2. *Nat. Rev. Immunol.* **20**, 392–394 (2020).
32. C. Atyeo, S. Fischinger, T. Zohar, M. D. Slein, J. Burke, C. Loos, D. J. McCulloch, K. L. Newman, C. Wolf, J. Yu, K. Shuey, J. Feldman, B. M. Hauser, T. Caradonna, A. G. Schmidt, T. J. Suscovich, C. Linde, Y. Cai, D. Barouch, E. T. Ryan, R. C. Charles, D. Lauffenburger, H. Chu, G. Alter, Distinct early serological signatures track with SARS-CoV-2 survival. *Immunity* **53**, 524–532.e4 (2020).
33. S. Khurana, S. Verma, N. Verma, C. J. Crevar, D. M. Carter, J. Manischewitz, L. R. King, T. M. Ross, H. Golding, Properly folded bacterially expressed H1N1 hemagglutinin globular head and ectodomain vaccines protect ferrets against H1N1 pandemic influenza virus. *PLOS ONE* **5**, e11548 (2010).
34. S. Khurana, E. M. Coyle, S. Verma, L. R. King, J. Manischewitz, C. J. Crevar, D. M. Carter, T. M. Ross, H. Golding, H5 N-terminal β sheet promotes oligomerization of H7-HA1 that induces better antibody affinity maturation and enhanced protection against H7N7 and H7N9 viruses compared to inactivated influenza vaccine. *Vaccine* **32**, 6421–6432 (2014).
35. S. Verma, M. Dimitrova, A. Munjal, J. Fontana, C. J. Crevar, D. M. Carter, T. M. Ross, S. Khurana, H. Golding, Oligomeric recombinant H5 HA1 vaccine produced in bacteria protects ferrets from homologous and heterologous wild-type H5N1 influenza challenge and controls viral loads better than subunit H5N1 vaccine by eliciting high-affinity antibodies. *J. Virol.* **86**, 12283–12293 (2012).
36. S. Ravichandran, M. Hahn, P. F. Belaunzarán-Zamudio, J. Ramos-Castañeda, G. Nájera-Cancino, S. Caballero-Sosa, K. R. Navarro-Fuentes, G. Ruiz-Palacios, H. Golding, J. H. Beigel, S. Khurana, Differential human antibody repertoires following Zika infection and the implications for serodiagnostics and disease outcome. *Nat. Commun.* **10**, 1943 (2019).
37. R. T. Davey Jr., E. Fernández-Cruz, N. Markowitz, S. Pett, A. G. Babiker, D. Wentworth, S. Khurana, N. Engen, F. Gordin, M. K. Jain, V. Kan, M. N. Polizzotto, P. Riska, K. Ruxrungtham, Z. Temesgen, J. Lundgren, J. H. Beigel, H. C. Lane, J. D. Neaton, R. T. Davey, E. Fernández-Cruz, N. Markowitz, S. Pett, A. G. Babiker, D. Wentworth, S. Khurana, N. Engen, F. Gordin, M. K. Jain, V. Kan, M. N. Polizzotto, P. Riska, K. Ruxrungtham, Z. Temesgen, J. Lundgren, J. H. Beigel, H. C. Lane, J. D. Neaton, J. Butts, E. Denning, A. DuChene, E. Krum, M. Harrison, S. Meger, R. Peterson, K. Quan, M. Shaughnessy, G. Thompson, D. Vock, J. Metcalf, R. Dewar, T. Rehman, V. Natarajan, R. McConnell, E. Flowers, K. Smith, M. Hoover, E. M. Coyle, D. Munroe, B. Aagaard, M. Pearson, A. Cursley, H. Webb, F. Hudson, C. Russell, A. Sy, C. Purvis, B. Jackson, Y. Collaco-Moraes, D. Carey, R. Robson, A. Sánchez, E. Finley, D. Conwell, M. H. Losso, L. Gambardella, C. Abela, P. Lopez, H. Alonso, G. Touloumi, V. Gioukari, O. Anagnostou, A. Avihingsanon, K. Pussadee, S. Ubolyam, B. Omotosho, C. Solórzano, T. Petersen, K. Vysyaraju, S. A. Rizza, J. A. Whitaker, R. Nahra, J. Baxter, P. Coburn, E. M. Gardner, J. A. Scott, L. Faber, E. Pastor, L. Makohon, R. A. MacArthur, L. M. Hillman, M. J. Farrough, H. M. Polenakovik, L. A. Clark, R. J. Colon, K. M. Kunisaki, M. DeConcini, S. A. Johnson, C. R. Wolfe, L. Mkumba, J. Y. Carbonneau, A. Morris, M. E. Fitzpatrick, C. J. Kessinger, R. A. Salata, K. A. Arters, C. M. Tasi, R. J. Panos, L. A. Lach, M. J. Glesby, K. A. Ham, V. G. Hughes, R. T. Schooley, D. Crouch, L. Muttera, R. M. Novak, S. C. Bleasdale, A. E. Zuckerman, W. Manosuthi, S. Thaonyen, T. Chiewcharn, G. Suwanpimolkul, S. Gatechumpol, S. Bunpasang, B. J. Angus, M. Anderson, M. Morgan, J. Minton, M. N. Gkamaletsou, J. Hambleton, D. A. Price, M. J. Llewelyn, J. Sweetman, J. Carbone, J. R. Arribas, R. Montejano, J. L. Lobo Beristain, I. Z. Martinez, J. Barberan, P. Hernandez, D. E. Dwyer, J. Kok, A. Borges, C. T. Brandt, L. S. Knudsen, N. Sypsas, C. Constantinou, A. Markogiannakis, S. Zakynthinos, P. Katsaounou, I. Kalomenidis, A. Mykietiuk, M. F. Alzogaray, M. Obed, L. M. Macias, J. Ebensrtejin, P. Burgoa, E. Nannini, M. Lahitte, S. Perez-Patrigeon, J. A. Martínez-Orozco, J. P. Ramírez-Hinojosa, Anti-influenza hyperimmune intravenous immunoglobulin for adults with influenza A or B infection (FLU-IVIG): A double-blind, randomised, placebo-controlled trial. *Lancet Respir. Med.* **7**, 951–963 (2019).
38. M. Sakharkar, C. G. Rappazzo, W. F. Wieland-Alter, C. L. Hsieh, D. Wrapp, E. S. Esterman, C. I. Kaku, A. Z. Wec, J. C. Geoghegan, J. S. McLellan, R. I. Connor, P. F. Wright, L. M. Walker,

Prolonged evolution of the human B cell response to SARS-CoV-2 infection. *Sci. Immunol.* **6**, eabg6916 (2021).
39. S. E. Benner, E. U. Patel, O. Laeyendecker, A. Pekosz, K. Littlefield, Y. Eby, R. E. Fernandez, J. Miller, C. S. Kirby, M. Keruly, E. Klock, O. R. Baker, H. A. Schmidt, R. Shrestha, I. Burgess, T. S. Bonny, W. Clarke, P. Caturegli, D. Sullivan, S. Shoham, T. C. Quinn, E. M. Bloch, A. Casadevall, A. A. R. Tobian, A. D. Redd, SARS-CoV-2 Antibody Avidity Responses in COVID-19 Patients and Convalescent Plasma Donors. *J. Infect. Dis.* **222**, 1974–1984 (2020).
40. J. Tang, G. Grubbs, Y. Lee, H. Golding, S. Khurana, Impact of convalescent plasma therapy on SARS CoV-2 antibody profile in COVID-19 patients. *Clin. Infect. Dis.* **2021**, ciab317 (2021).
41. N. Kaneko, H.-H. Kuo, J. Boucau, J. R. Farmer, H. Allard-Chamard, V. S. Mahajan, A. Piechocka-Trocha, K. Lefteri, M. Osborn, J. Bals, Y. C. Bartsch, N. Bonheur, T. M. Caradonna, J. Chevalier, F. Chowdhury, T. J. Diefenbach, K. Einkauf, J. Fallon, J. Feldman, K. K. Finn, P. Garcia-Broncano, C. A. Hartana, B. M. Hauser, C. Jiang, P. Kaplonek, M. Karpell, E. C. Koscher, X. Lian, H. Liu, J. Liu, N. L. Ly, A. R. Michell, Y. Rassadkina, K. Seiger, L. Sessa, S. Shin, N. Singh, W. Sun, X. Sun, H. J. Ticheli, M. T. Waring, A. L. Zhu, G. Alter, J. Z. Li, D. Lingwood, A. G. Schmidt, M. Lichterfeld, B. D. Walker, X. G. Yu, R. F. Padera Jr., S. Pillai; Massachusetts Consortium on Pathogen Readiness Specimen Working Group, Loss of Bcl-6-expressing T follicular helper cells and germinal centers in COVID-19. *Cell* **183**, 143–157.e13 (2020).
42. D. Wrapp, N. Wang, K. S. Corbett, J. A. Goldsmith, C. L. Hsieh, O. Abiona, B. S. Graham, J. S. McLellan, Cryo-EM structure of the 2019-nCoV spike in the prefusion conformation. *Science* **367**, 1260–1263 (2020).
43. J. Tang, Y. Lee, S. Ravichandran, G. Grubbs, C. Huang, C. B. Stauft, T. Wang, B. Golding, H. Golding, S. Khurana, Epitope diversity of SARS-CoV-2 hyperimmune intravenous human immunoglobulins and neutralization of variants of concern. *iScience* **24**, 103006 (2021).

Acknowledgments: We thank K. Peden and M. Zaitseva for insightful review of the manuscript. **Funding:** The antibody characterization work described here was supported by FDA intramural grant funds and NIH-NIAID IAA no. AAI20040 and FDA's Medical Countermeasures Initiative (MCMi) grant no. OCET 2021-1565. The funders had no role in study design, data collection and analysis, decision to publish, or preparation of the manuscript. The content of this publication does not necessarily reflect the views or policies of the Department of Health and Human Services nor does mention of trade names, commercial products, or organizations imply endorsement by the U.S. government. **Author contributions:** S.K. conceived and designed research; S.R., G.G., J.T., Y.L. and C.H. performed research; and H.G. and S.K. contributed to writing. All authors discussed the results and commented on the manuscript. **Competing interests:** The authors declare that they have no financial or other competing interests. **Data and materials availability:** All data needed to evaluate the conclusions in the paper are present in the paper and/or the Supplementary Materials. The materials generated during the current study are available from the lead contact under a material transfer agreement on reasonable request.

Submitted 22 March 2021
Accepted 23 August 2021
Published 13 October 2021
10.1126/sciadv.abi6533

Citation: S. Ravichandran, G. Grubbs, J. Tang, Y. Lee, C. Huang, H. Golding, S. Khurana, Systemic and mucosal immune profiling in asymptomatic and symptomatic SARS-CoV-2–infected individuals reveal unlinked immune signatures. *Sci. Adv.* **7**, eabi6533 (2021).